JOURNAL OF CATALYSIS 113, 434–443 (1988)

The Effects of the Local Concentration and Distribution of Sulfonic Acid Groups on 1-Butene Isomerization Catalyzed by Macroporous Ion-Exchange Resin Catalysts

J. H. AHN, S. K. IHM,[1] AND K. S. PARK

Department of Chemical Engineering, Korea Advanced Institute of Science and Technology, P.O. Box 131, Cheongryang, Seoul, Korea

Received December 22, 1987; revised April 15, 1988

The catalytic activities of sulfonated macroporous poly(styrene–divinylbenzene) beads in 1-butene isomerization were investigated through a model concerning the effects of the distribution and concentration of the sulfonic acid groups. The reaction rate constant increased nonlinearly with the sulfonic acid group concentration and the order of nonlinear power dependence was about 2.4. The values of effectiveness factors of the microparticles in the macroporous resin catalysts with 40 and 50% DVB ranged from 0.1 to 0.3. The diffusivities were 10^{-13} and 10^{-14} cm^2/sec for 40 and 50% DVB, respectively. The result showed that the major reaction arena was the pore space between the microparticles. © 1988 Academic Press, Inc.

INTRODUCTION

Macroporous resins consist of agglomerates of the polymer gel particles interdispersed with macropores (*1*). Macroporous resins have two kinds of functional groups: one on the surface of gelular microparticle and the other inside the gelular phase. The fraction of the surface functional groups from the total amount can be controlled by several variables such as the synthetic conditions of the macroporous resin bead and functionalization method. The catalytic activity of macroporous resin catalysts with higher crosslinking strongly depends on the functional group distribution within the microparticles because of the diffusion limitation in the gelular microparticle.

For a sulfonic acid resin catalyst, catalytic function is due to the ensembles of several $-SO_3H$ groups in nonaqueous medium (*2–4*) and catalytic activity increases nonlinearly with the increasing concentration of sulfonic acid groups (*3, 5–7*).

Klein *et al.* (*8*) demonstrated that the distribution of the sulfonic acid groups within the resin catalysts could be controlled so that different concentration profiles were obtained, and the properties and reaction behavior of the resin catalysts were varied to a large extent by the local concentration and distribution of the sulfonic acid groups. Chee and Ihm (*9*) showed that the distribution of sulfonic acid groups within the microparticles of the macroporous sulfonic acid resins affected the deactivation patterns of the catalysts when they were used in ethanol dehydration. Although the local concentration and distribution of the functional groups have become important factors, few investigations have been made to explain the effects of these factors on the catalytic activity. Accordingly it is desirable to study more systematically the effect of the local concentration and distribution of functional groups on the catalytic activity. However, the results obtained can be complicated by interactions with solvents and in addition by polymer swelling. If highly crosslinked resins are used in nonpolar medium, these effects can be sup-

[1] To whom all correspondence should be addressed.

0021-9517/88 $3.00

pressed. Polymeric acid catalysts used in such a system involve the isomerization of olefins (*5*, *10*) or the alkylation of benzene with olefins (*11*, *12*).

The purpose of this work is to extend the two-phase model (*13*, *14*) to the resin catalyst with an inhomogeneous distribution of functional groups and to apply the model to analyze the effect of the local concentration and distribution of the functional groups on the catalytic activity. This includes a breakdown of the effect of the gel-phase permeation on the reaction rate. The macroporous poly(styrene–co-divinylbenzene) resin catalysts with an inhomogeneous distribution of sulfonic acid groups were prepared and their catalytic activities in 1-butene isomerization were analyzed through the proposed model.

THEORY

For a given polymer bead, the functional group distribution varies with the reaction conditions in the functionalization. In the case of gelular resin beads which are accessible only by swelling, the distribution of functional groups can be easily observed by X-ray energy dispersive analysis (EDAX). On the other hand the rate of functionalization for a macroporous resin bead is affected not only by the diffusion in the macropores but also by the gelular permeation through the microparticles (*15*).

The capacity of acid resin catalysts is usually measured by the titration method. The capacity measured in such a way is the value averaged over the entire bead volume and it does not explain the functional group distribution in full. The measured capacity, e, for a gelular microparticle is related to the local capacity level C_L as

$$e = \frac{\int_0^{R_i} 4\pi r_i^2 C_L(r_i) dr_i}{(4/3)\pi R_i^3}, \qquad (1)$$

where the units of both e and C_L are taken as milliequivalents per unit mass of unsulfonated polymer matrix and R_i is the radius of a gelular microparticle as shown in Fig. 1.

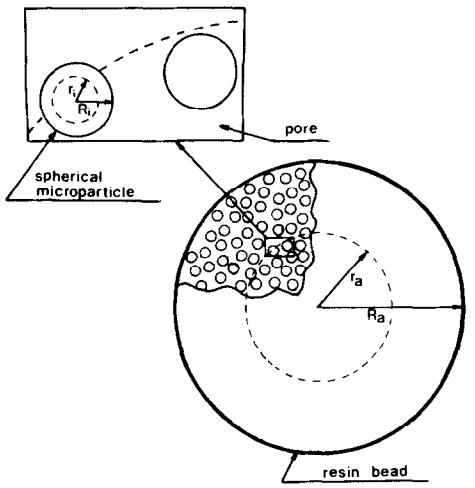

FIG. 1. The schematic diagram of a macroporous resin bead.

As far as the functional group distribution is concerned, it implies that the local capacity level is a function of radial position, i.e., $C_L(r_i)$. Because the present work is aimed at analyzing the effect of different functional group distributions on the catalytic activity, it will be more straightforward to start with rather simple distributions. Therefore, three types of functional group distribution can be postulated as shown in Fig. 2.

Type A distribution is a complete sulfonation with uniform local capacity level C_L^0. The distribution of type B can be ob-

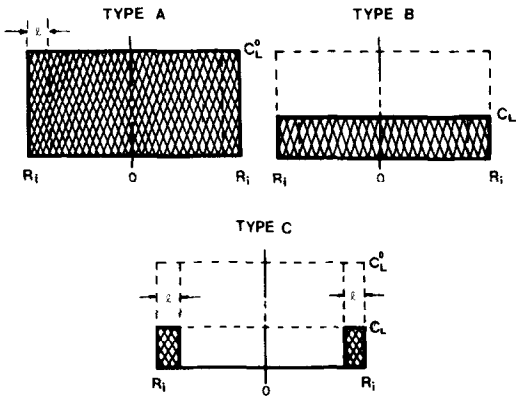

FIG. 2. The schematic diagrams for three types of functional group distribution.

tained from type A through ion exchange with Na^+ ion, which results in uniform deactivation (*8*).

For the type C distribution all the functional groups are located only on the surface of the microparticle. If γ is defined as the ratio of the capacity of external functional groups located on the surface of the microparticle, which provide easy access to the reactants without penetration through the polymer matrix, to the total capacity,

$$\gamma = \frac{e_\gamma}{e}. \tag{2}$$

In order to know the external capacity, e_γ, it will be necessary to know the characteristic depth of the external layer of sulfonated polymer matrix. If the depth is defined as l, e_γ can be expressed by

$$e_\gamma = \frac{\int_{R_i - l}^{R_i} 4\pi r_i^2 C_L dr_i}{(4/3)\pi R_i^3} = C_L\left[1 - \left(1 - \frac{l}{R_i}\right)^3\right]. \tag{3}$$

For complete sulfonation, type A,

$$e_\gamma^0 = C_L^0\left[1 - \left(1 - \frac{l}{R_i}\right)^3\right], \tag{4}$$

where C_L^0 is the local capacity per unit mass of unsulfonated polymer matrix for fully sulfonated catalyst. In the case of type C where all the functional groups are located on the surface, γ is equal to 1. For the distribution of type B, it can be written as

$$\gamma = \frac{e_\gamma}{e} = \frac{C_L[1 - (1 - l/R_i)^3}{C_L} = \frac{e_\gamma^0}{C_L^0} = \frac{e_\gamma^0}{e_m} = \gamma^0. \tag{5}$$

This implies that the resin catalyst with a uniform distribution such as type A or B has the constant value of γ^0 which does not depend on the capacity level but on the physical properties of the polymer matrix. The value of γ^0 corresponds to that of complete sulfonation.

Since it is very difficult in reality to know the value of l, setting a standard experimental technique measuring e_γ is preferred. Prokop and Setinek (*16, 17*) carried out the adsorption and desorption of ammonia to understand the accessibility of the functional groups in a series of ion-exchange resins with varying degrees of crosslinking of the basic copolymer. They demonstrated that on desorption into a gaseous phase under reduced pressure, ammonia was released only from functional groups located on the surface of ion-exchange resin and then the amount of desorbed ammonia was proportional to the surface area of ion-exchange resin in the initial stage (3–4 hr). Therefore, it is considered that e_γ can be measured experimentally.

It can be shown that the local capacity level is expressed in terms of measurables as

$$\begin{aligned} &\text{Type A:} \quad C_L = e_m \\ &\text{Type B:} \quad C_L = e \\ &\text{Type C:} \quad C_L = e/\gamma^0. \end{aligned} \tag{6}$$

There are still many uncertainties about the effect of the local capacity level of the functional groups on the catalytic activity for sulfonated porous resin. According to Gates *et al.* (*3*) and Jerabek *et al.* (*4*), it has been proposed that the reaction rate constant per unit mass of sulfonated polymer catalyst has a power dependence on the local capacity level in the unit of milliequivalents per unit mass of sulfonated polymer matrix, i.e.,

$$k_v' = k_0'(C_L'/C_L^{0\prime})^m, \tag{7}$$

where k_0' is the reaction rate constant per unit mass of fully sulfonated polymer matrix. Jerabek *et al.* (*4*) demonstrated that m was the number of the active sites participating in the rate-determining step of *t*-butyl alcohol dehydration. The unit of the local capacity level can be easily converted for its appropriate applications. For example, if C_L, milliequivalents per g of unsulfonated polymer matrix, corresponds to C_L', milliequivalents per g_s of sulfonated poly-

mer matrix, they are related to each other as

$$C_L' = \frac{1}{1/C_L + 0.08}. \quad (8)$$

Accordingly C_L', milliequivalents per g_s of sulfonated polymer matrix, can be expressed as

$$\text{Type A:} \quad C_L' = \frac{1}{1/e_m + 0.08} = e_m'$$

$$\text{Type B:} \quad C_L' = \frac{1}{1/e + 0.08} = e' \quad (9)$$

$$\text{Type C:} \quad C_L' = \frac{1}{\gamma^0/e + 0.08}.$$

According to the two-phase model for a porous resin catalyst, the external functional groups can take part in the catalytic reaction without the gel-phase permeation while the internal ones can be available only through the gel-phase permeation (*13, 14*). Accordingly the overall effectiveness factor can be expressed in terms of the fraction of functional groups on the external surface, the macro- and the micro-effectiveness factors. γ is considered a weight factor for the contribution of external functional groups and $(1 - \gamma)\bar{\eta}_i$ that of internal functional groups to the reaction,

$$\eta_{ov} = \eta_a[\gamma + (1 - \gamma)\bar{\eta}_i], \quad (10)$$

where $\bar{\eta}_i$ is the micro-effectiveness factor and its analytic solution can be obtained for a first-order irreversible reaction as

$$\bar{\eta}_i = \frac{3}{m_i}\left(\frac{1}{\tanh m_i} - \frac{1}{m_i}\right), \quad (11)$$

where $m_i = R_i\sqrt{k_v'/D_i}$.

Because the above concept is based on the unit functional group, its application to the overall reaction rate requires the same basis. Without pore diffusional limitation ($\eta_a = 1$), the overall rate constant per unit capacity is written as

$$k_{ov} = k_v[\gamma + (1 - \gamma)\bar{\eta}_i], \quad (12)$$

where $k_v = k_v'/e'$.

The intrinsic rate constant k_v can be expressed as

$$\text{Type A:} \quad k_v = \frac{k_0'}{e_m'}; \quad \bar{\eta}_i(m_i^0)$$

$$\text{Type B:} \quad k_v = \frac{k_0'}{e'}\left(\frac{e'}{e_m'}\right)^m; \quad \bar{\eta}_i(m_i) \quad (13)$$

$$\text{Type C:} \quad k_v = \frac{k_0'}{e'}\left[\frac{(\gamma^0/e + 0.08)^{-1}}{e_m'}\right]^m; \quad \gamma = 1,$$

where $m_i^0 = R_i\sqrt{k_0'/D_i}$.

Experiments for the aforementioned model can be designed such that there is no pore diffusional limitation for a porous resin catalyst with sufficiently small bead sizes. External mass transfer resistance can be eliminated by controlling the stirring speed for a batch reactor or by increasing the flow rate for a fixed-bed reactor. Also, a first-order kinetics can be assured in most cases by carrying out the reaction in the sufficiently low range of reactant concentration. The initial reaction rates obtained under such conditions are controlled only by the kinetics and the gel-phase permeation. It is hoped by analyzing such initial reaction rates that the effect of gel-phase permeation can be isolated and also that the dependence of the rate constant on the local capacity level can be understood. First, through the type C catalyst, one can easily obtain the intrinsic rate constant k_0' and the association number m. With k_0' and m known, the micro-effectiveness factor can be estimated for the catalysts with other type distributions. Then the gelular permeability, D_i, can be calculated.

EXPERIMENTAL

Preparation of Poly(styrene–divinylbenzene) Beads

Macroporous styrene–divinylbenzene copolymer beads were prepared by a suspension polymerization with two crosslinking degrees of 40 and 50%. The suspension

copolymerization was carried out in a standard polymerization apparatus, consisting of a 1-liter four-necked round-bottomed flask fitted with a variable mechanical stirrer, a thermometer, a nitrogen inlet, and a reflux condenser. The aqueous phase consisted of 600 g of distilled water, 1.6 g of boric acid, 9 g of poly(diallyldimethylammonium chloride) aqueous solution (15%), and 1.5 g of gelatin. After the aqueous phase was thoroughly mixed, the pH was controlled within the range 8.3 to 8.7 by the addition of 50% aqueous NaOH (*18*).

The monomer phase consisted of 40 ml of styrene and divinylbenzene (40 or 50% crosslinking), 60 ml of toluene as diluent, and 0.9 g of α,α'-azobisisobutyronitril as initiator. The monomer mixture was dispersed as fine droplets in aqueous phase and the copolymerization was carried out at 80°C for about 12 hr in a thermostated water bath.

The polymer beads obtained were filtered, washed, extracted with acetone in a Soxhlet apparatus, and dried under vacuum.

The same procedures without the addition of toluene resulted in gelular beads.

Sulfonation of Polymer Beads

The macroporous resin beads were sulfonated by different methods to give different sulfonic acid group distributions.

Type A or B. The resin catalyst with homogeneous distribution can usually be obtained by sulfonation in a proper swelling medium. The beads were swollen with 1,2-dichloroethane and then sulfonated with concentrated sulfuric acid at 95°C for 32 hr. The sulfonated beads were hydrated very slowly with deionized water, predried in a drying oven at 70°C, and then dried thoroughly at 110°C under vacuum for 48 hr. The macroporous resin catalysts with lower acid group concentrations were obtained from fully saturated catalysts by partial neutralization with aqueous NaOH.

Type C. Twenty-five milliliters of concentrated sulfuric acid, 32 ml of 1,2-dichloroethane, and 92 ml of nitrobenzene were well mixed in a 250-ml Erlenmeyer flask. About 5 g of the macroporous resin beads was added to the mixture and sulfonated at 25°C. The sulfonated beads were transferred to a 1000-ml Erlenmeyer flask at an appropriate time and then hydrated slowly. The hydrated resin catalysts were dried as described above.

The capacity of sulfonic acid groups in the resin catalyst was measured by titration. The macrodistribution of sulfonic acid groups in the resin catalyst was directly observed by X-ray energy dispersive analysis using a scanning electron microscope (Hitachi S 550). The physical properties of the macroporous resin catalysts with the type A distribution were listed in Table 1. It should be noted here that the microdistribution of sulfonic acid groups in a microparticle with a diameter of about 10^{-6} cm could not be observed even with EDAX.

Activity Measurement

The catalytic activity of 1-butene isomerization was measured at 95°C by using a glass flow reactor system. The appropriate amounts of catalysts were transferred from the vacuum oven to the reactor. 1-Butene and nitrogen were passed through the oxygen and moisture traps to remove oxygen and water, respectively. 1-Butene was fed to a gas mixer, in which it was mixed with nitrogen and then introduced to the reactor. The reactor was provided with a thermocouple well and placed in a temperature-

TABLE 1

Physical Properties of the Macroporous Resin Catalysts with the Type A Distribution

Properties	% DVB	
	40	50
Microparticle density (g_s/cm)[a]	1.40	1.40
Surface area (m^2/g_s)	200	300
Avg. microparticle diameter (cm)	2.14×10^{-6}	1.43×10^{-6}
Ion-exchange capacity (meq/g_s) e'_m	3.42	3.26
Fraction of $-SO_3H$ groups on microparticle surfaces (γ^0)[a]	0.23	0.27

[a] The values were assumed from Refs. (*16, 17*).

controlled oil bath. Reaction products were analyzed periodically by gas chromatography with a 9-m-long, $\frac{1}{8}$-in.-diameter stainless-steel column packed with 7% Squalane on Chromosorb P.

RESULTS AND DISCUSSION

The distribution of sulfonic acid groups was directly observed by EDAX.

Figure 3a showed the homogeneous distribution of the sulfonic acid groups in the type A macroporous catalyst with 40% crosslinking which was sulfonated completely with concentrated H_2SO_4 at 95°C. The decreased concentration of the sulfonic acid groups was obtained by ion exchange with Na^+ ion of the type A catalyst. The homogeneous distribution was also confirmed by EDAX as shown in Fig. 3b. Therefore the profiles of sulfonic acid groups were known to be uniform across the bead and the Na^+ exchange process worked as expected to lower the concentration of sulfonic acid groups uniformly.

It can be expected that inhomogeneous distribution is to be obtained by partial sulfonation of the resin beads. In the case of the sulfonation with $H_2SO_4/C_2H_4Cl_2/C_6H_5NO_2$ at 25°C for 7 and 20 hr, the absence of the macropore diffusion limitation during the sulfonation was verified by a quasi-homogeneous distribution of the sulfonic acid groups throughout the entire bead as shown in Fig. 4. This does not mean that the sulfonic acid group distribution inside the gelular microparticles is homogeneous. Unfortunately the distribution in the microparticles cannot be observed directly due to their very small sizes (10^{-6} cm). Therefore, the gelular resin beads with the same crosslinking were used as the counterparts.

In the case of functionalization of gelular beads it is known that the interior is accessible only by swelling. The swelling of the 40% crosslinked gelular bead was not observed under the sulfonation conditions. The sulfur content could not be detected by EDAX as shown in Fig. 5. The sulfonation

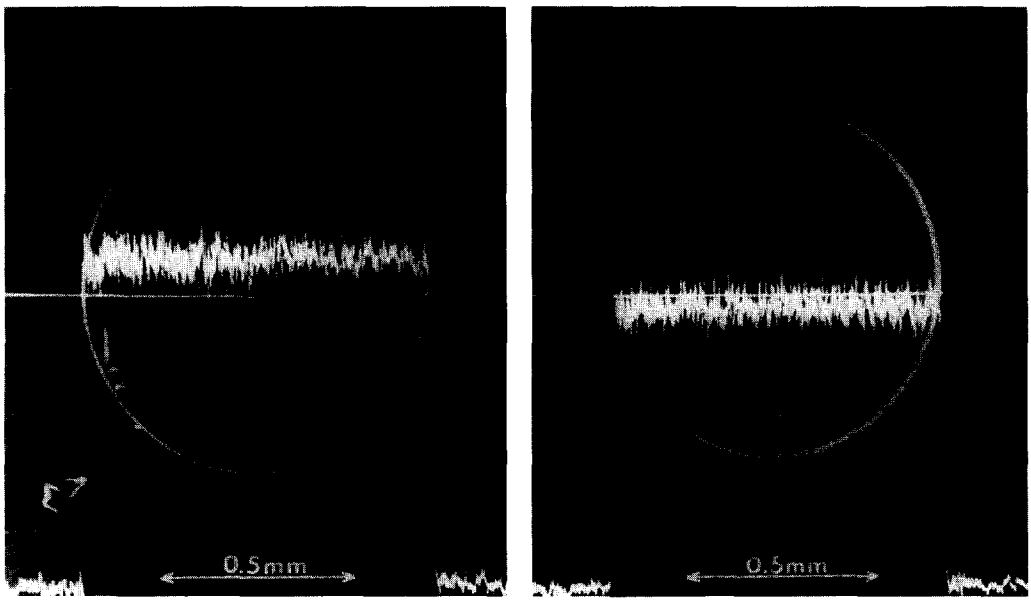

FIG. 3. Electron micrographs of the sulfur profile within the porous bead sulfonated with $H_2SO_4/C_2H_4Cl_2$ at 95°C (magnification factor = 2.5×10^3). (a) Completely sulfonated; (b) ion-exchanged with Na^+.

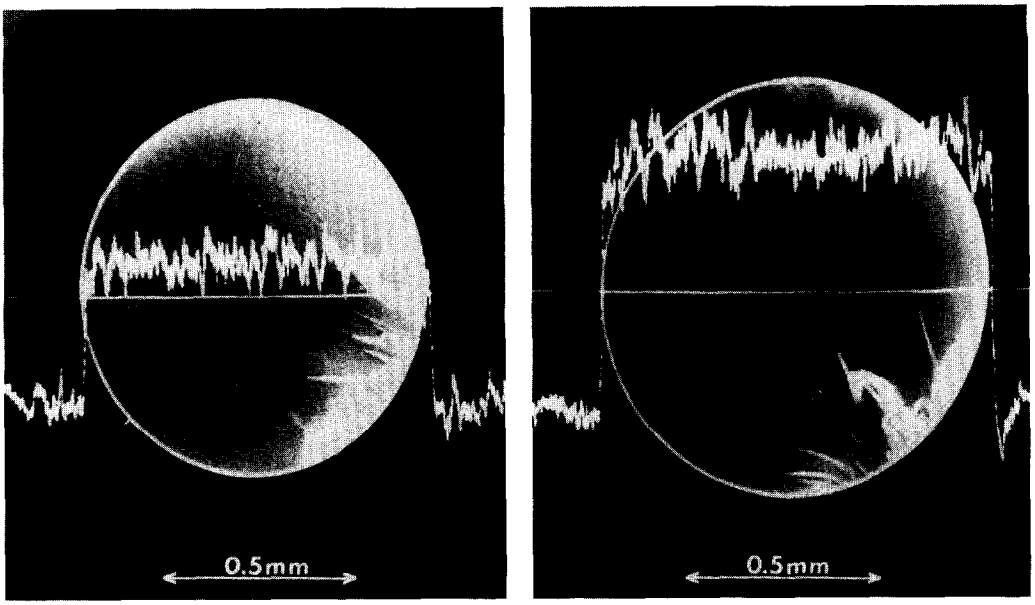

FIG. 4. Electron micrographs of the sulfur profile within the porous bead sulfonated with H_2SO_4/$C_2H_4Cl_2$/$C_6H_5NO_2$ at 25°C (magnification factor = 5×10^2). (a) Sulfonation time = 7 hr; (b) sulfonation time = 20 hr.

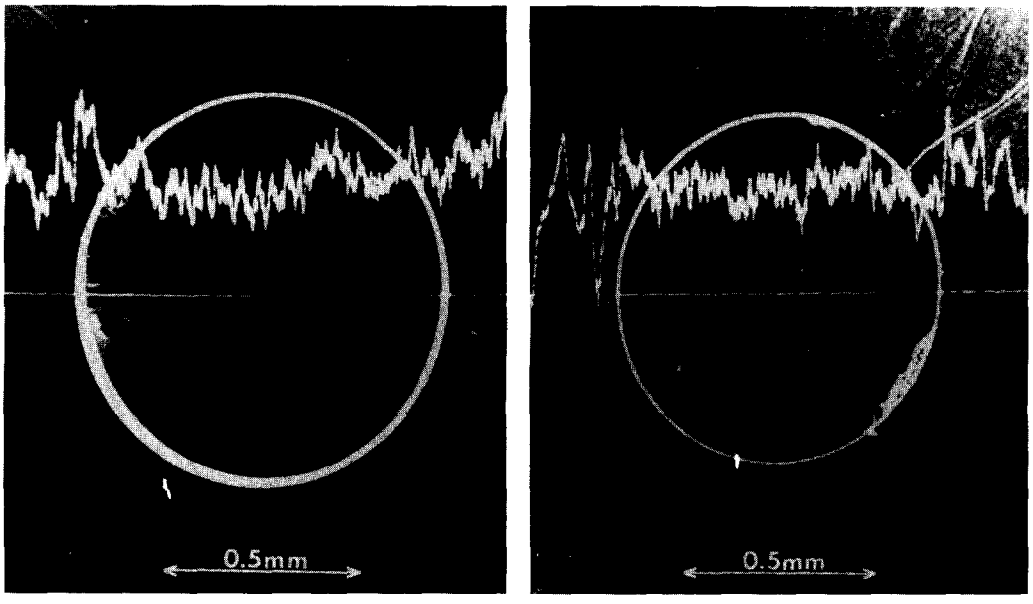

FIG. 5. Electron micrographs of the sulfur profile within the gelular bead sulfonated with H_2SO_4/$C_2H_4Cl_2$/$C_6H_5NO_2$ at 25°C (magnification factor = 2.5×10^2). (a) Sulfonation time = 7 hr; (b) sulfonation time = 20 hr.

reaction, however, could be assured by observing the color change of bead surface as well as by the small ion-exchange capacity of the sulfonated bead. The sulfonation of the gelular bead would take place only at the surface. Similarly it is considered that the sulfonic acid groups in the macroporous resin bead will be located only on the surface of the microparticles. Accordingly in the case of the sulfonation with H_2SO_4/$C_2H_4Cl_2$/$C_6H_5NO_2$ at 25°C the resulting distribution may be classified as type C.

Initial reaction rates were determined as a slope of the conversion versus space velocity (W/F); in most cases these dependences were linear within the range of the conversions obtained. Preliminary experiments carried out with varying feed flow rate at a constant space velocity revealed that the influence of the external mass transfer was negligible within the range used. It was ascertained from the observed reaction rates obtained with varying particle sizes of the catalysts that the pore diffusion limitation was negligible.

The observed rate constants were calculated from a Langmuir-type equation for low partial pressures,

$$r'_{ov} = \frac{k'K_A x}{1 + K_A x} = \frac{k'_{ov} x}{1 + K_A x} \sim k'_{ov} x. \quad (14)$$

For the type C distribution, the change of catalytic activities was depicted with different ion-exchange capacities as shown in Fig. 6. The catalytic activity increased nonlinearly with ion-exchange capacity and the catalytic activity of 40% crosslinking was greater than that of 50% crosslinking. In the case of the type C distribution ($\gamma = 1$), the following equation can be obtained from Eqs. (9) and (13):

$$k'_{ov} = k'_v = k'_0(C'_L/e'_m)^m. \quad (15)$$

With the same bead capacity e, the value of C'_L becomes larger with lower value of γ^0 as indicated in Eq. (9). Therefore the lower crosslinking (40%) with lower value of γ^0 will result in higher value of rate constants.

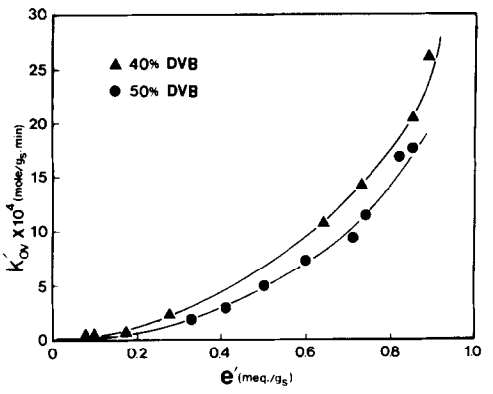

FIG. 6. Effect of ion-exchange capacity on catalytic activity of resin catalysts with the type C distribution.

Taking the logarithm of Eq. (15) gives

$$\ln k'_{ov} = m \ln C'_L + \ln(k'_0/e'^m_m).$$

The logarithmic plot of k'_{ov} versus C'_L will provide m from the slope and k'_0 from the intercept at $C'_L = 1$. The values of m and k'_0 were obtained from Fig. 7 and the intrinsic rate constant k'_v could be related to the local capacity level C'_L as

$$k'_v = (2.9 \times 10^{-3})(C'_L/3.42)^{2.4} \text{ (mol/}g_s \cdot \text{ min) for 40\% DVB}$$

$$k'_v = (2.6 \times 10^{-3})(C'_L/3.26)^{2.4} \text{ (mol/}g_s \cdot \text{ min) for 50\% DVB.} \quad (16)$$

For the type B distribution, the catalytic activity increased with ion-exchange capacity as shown in Fig. 8. The ion-exchange

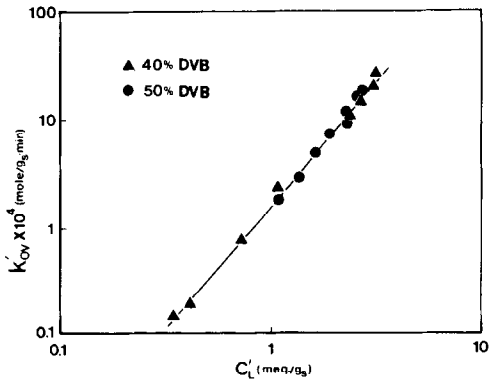

FIG. 7. Change of the catalytic activity with local capacity level of the type C distribution.

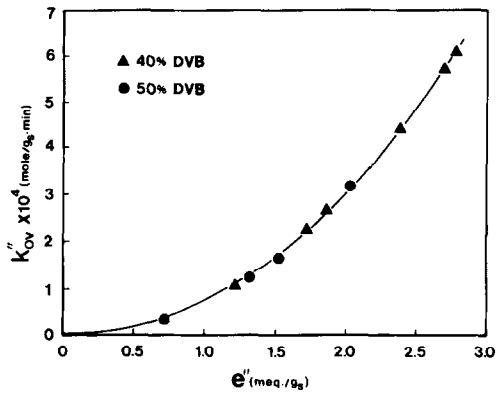

FIG. 8. Effect of ion-exchange capacity on catalytic activity of resin catalysts with the type B distribution.

capacity e'' was expressed in terms of sulfonated polymer matrix excluding the mass of Na^+. This was needed because the type B catalysts were obtained through uniform deactivation with Na^+ from the type A catalyst. From Eqs. (12) and (13), the following equation can be derived,

$$k'_{ov} = k'_v[\gamma + (1 - \gamma)\bar{\eta}_i]; \quad \bar{\eta}_i[m_i(k'_v, D_i)]. \quad (17)$$

Since the value of k'_v was already known from Eq. (16), $\bar{\eta}_i$ could be obtained and in turn m_i and D_i could be obtained. The values were listed in Table 2.

The effectiveness factor decreased with ion-exchange capacity. It was considered because the Thiele modulus $m_i(k'_v, D_i)$ increased as the intrinsic rate constant k'_v increased nonlinearly with ion-exchange capacity. The effectiveness factors ranged from 0.1 to 0.3, and the diffusivities were $\sim 10^{-13}$ cm^2/sec for 40% DVB and $\sim 10^{-14}$ cm^2/sec for 50% DVB. It is believed from the results that the major reaction arena is the pore space between the microparticles.

CONCLUSIONS

A model has been proposed to analyze the effect of the distribution and local concentration of functional groups on the catalytic activity. The macroporous resin beads were sulfonated to have different distributions of the sulfonic acid groups. The catalytic activities of 1-butene isomerization were measured by using the sulfonated resin catalysts and analyzed through the model.

The catalytic activity increased nonlinearly with the sulfonic acid group concentration and the order was about 2.4. Accordingly the number of sulfonic acid groups participating in the rate-determining step of 1-butene isomerization seems to be $2 \sim 3$.

The intrinsic rate constant is related to the local concentration of the sulfonic acid groups as

$$k'_v = (2.9 \times 10^{-3})(C'_L/3.42)^{2.4} \quad (\text{mol}/g_s \cdot \text{min}) \text{ for 40\% DVB}$$

$$k'_v = (2.6 \times 10^{-3})(C'_L/3.26)^{2.4} \quad (\text{mol}/g_s \cdot \text{min}) \text{ for 50\% DVB.}$$

The values of the effectiveness factors in the microparticles range from 0.1 to 0.3. This indicates that the major reaction arena

TABLE 2

Effectiveness Factors of Microparticles in the Macroporous Resin Catalysts with the Type B Distribution

% DVB	e' (meq/g_s)	k'_{ov} (mol/g_s · min)	e (meq/g_s)	e'' (meq/g_s)	k''_{ov} (mol/g_s · min)	k'_v (mol/g_s · min)	$\bar{\eta}_i$	m_i	D_i (cm^2/sec)
40	0.92	8.21×10^{-5}	1.34	1.21	1.08×10^{-4}	2.45×10^{-4}	0.27	10.0	1.1×10^{-13}
	1.39	1.82×10^{-4}	2.00	1.72	2.26×10^{-4}	5.67×10^{-4}	0.22	12.5	1.6×10^{-13}
	1.53	2.88×10^{-4}	2.19	1.86	2.65×10^{-4}	6.83×10^{-4}	0.21	13.2	1.7×10^{-13}
	2.07	3.85×10^{-4}	2.94	2.38	4.42×10^{-4}	1.23×10^{-3}	0.17	16.6	2.0×10^{-13}
	2.45	5.20×10^{-4}	3.45	2.70	5.73×10^{-4}	1.66×10^{-3}	0.15	18.9	2.1×10^{-13}
	2.56	5.80×10^{-4}	3.59	2.79	6.10×10^{-4}	1.79×10^{-3}	0.14	20.4	1.9×10^{-13}
50	0.53	2.35×10^{-5}	0.76	0.72	3.20×10^{-5}	7.12×10^{-5}	0.25	10.9	1.2×10^{-14}
	1.04	9.78×10^{-5}	1.47	1.32	1.24×10^{-4}	3.01×10^{-4}	0.19	14.7	2.8×10^{-14}
	1.23	1.34×10^{-4}	1.74	1.53	1.66×10^{-4}	4.28×10^{-4}	0.16	17.7	2.7×10^{-14}
	1.74	2.71×10^{-4}	2.43	2.03	3.16×10^{-4}	8.39×10^{-4}	0.15	18.9	4.6×10^{-14}

in 1-butene isomerization is the pore space between the microparticles.

APPENDIX: NOMENCLATURE

C_L local concentration of functional groups based on unsulfonated polymer matrix; C_L^0, when saturated, meq/g.

C_L' local concentration of functional groups based on sulfonated polymer matrix; $C_L^{0\prime}$, when saturated, meq/g_s.

D_i diffusivity in the gelular microparticle, cm^2/sec.

e measured capacity based on unsulfonated polymer matrix; e_m, when saturated; e_γ, the capacity of external functional groups; e_γ^0, the capacity of external functional groups when saturated, meq/g.

e' measured capacity based on sulfonated polymer matrix, meq/g_s.

F molar flow rate of 1-butene, mol/min.

g mass of unsulfonated polymer matrix, g.

g_s mass of sulfonated polymer matrix, g.

k reaction rate constant based on milliequivalents of functional groups; k_{ov}, observed; k_v, intrinsic, mol/meq · min.

k' reaction rate constant based on unit mass of sulfonated polymer matrix; k_{ov}' observed; k_v', intrinsic, mol/g_s · min.

K_A adsorption constant in Eq. (14).

l depth of the external layer, cm.

m power for Eq. (7).

m_i Thiele modulus, dimensionless.

r_i radial position from the center of a gelular microparticle, cm.

R_i radius of a gelular microparticle, cm.

W mass of the sulfonated resin catalysts loaded, g_s.

x mole fraction of 1-butene, dimensionless.

γ fraction of functional groups distributed over the pore walls; γ^0, when saturated, dimensionless.

η effectiveness factor; $\bar{\eta}_i$, for a microparticle; η_a, for the pore space; η_{ov}, for a resin bead, dimensionless.

ACKNOWLEDGMENTS

This work has been carried out as a cooperative research between KAIST of Korea and Technical University of Braunschweig of West Germany. The authors acknowledge financial support from the Korea Ministry of Science and Technology and the Korea Science and Engineering Foundation. Dr. H. Widdecke of Institut für Technische Chemie of T.U. Braunschweig is especially acknowledged for his cooperation and helpful discussions throughout this work.

REFERENCES

1. Pitochelli, A. R., "Ion-Exchange Catalysis and Matrix Effect." Rohm & Haas, Philadelphia, 1975.
2. Thornton, R., and Gates, B. C., *J. Catal.* **34,** 275 (1974).
3. Gates, B. C., Wisnouskas, J. S., and Heath, H. W., Jr., *J. Catal.* **24,** 320 (1972).
4. Jerabek, K., Bazant, V., Beranek, L., and Setinek, K., *in* "Proceedings, 5th International Congress on Catalysis, Palm Beach, 1972" (J. W. Hightower, Ed.), pp. 1193–1203. North-Holland, Amsterdam, 1973.
5. Uematsu, T., *Bull. Chem. Soc. Japan* **45,** 3329 (1972).
6. Ancillotti, F., Mauri, M. M., and Pescarollo, E., *J. Catal.* **46,** 49 (1977).
7. Jerabek, K., and Setinek, K., *J. Mol. Catal.* **39,** 161 (1987).
8. Klein, J., Widdecke, H., and Bothe, N., *Makromol. Chem. Suppl.* **6,** 211 (1984).
9. Chee, Y. C., and Ihm, S. K., *J. Catal.* **102,** 180 (1986).
10. Tsuchiya, S., and Ozaki, A., *J. Catal.* **5,** 537 (1966).
11. Wesley, R. B., and Gates, B. C., *J. Catal.* **34,** 288 (1974).
12. Buttersack, S., Widdecke, H., and Klein, J., *J. Mol. Catal.* **40,** 23 (1987).
13. Ihm, S. K., Suh, S. S., and Oh, I. H., *J. Chem. Eng. Japan* **15,** 206 (1982).
14. Ihm, S. K., and Oh, I. H., *J. Chem. Eng. Japan* **17,** 58 (1984).
15. Ihm, S. K., Ahn, J. H., Widdecke, H., Struβ, K., and Klein, J., *J. Appl. Polym. Sci.*, in press.
16. Prokop, Z., and Setinek, K., *J. Polym. Sci. Polym. Chem. Ed.* **12,** 2535 (1974).
17. Prokop, Z., and Setinek, K., *J. Polym. Sci. Polym. Chem. Ed.* **12,** 2545 (1974).
18. Minkiewicz, J. V., Milstein, D., Lieto, J., Gates, B. C., and Albright, R. L., "Chemically Modified Surfaces in Catalysis and Electrocatalysis" (J. S. Miller, Ed.), ACS Symposium Series No. 192, pp. 9–29. Amer. Chem. Soc., Washington, DC, 1982.